2024 American Control Conference (ACC)
July 8-12, 2024. Toronto, Canada

Safe Optimal Interactions Between Automated and Human-Driven Vehicles in Mixed Traffic with Event-triggered Control Barrier Functions

Anni Li, Christos G. Cassandras and Wei Xiao

Abstract— **This paper studies safe driving interactions between Human-Driven Vehicles (HDVs) and Connected and Automated Vehicles (CAVs) in mixed traffic where the dynamics and control policies of HDVs are unknown and hard to predict. In order to address this challenge, we employ event-triggered Control Barrier Functions (CBFs) to estimate the HDV model online, construct data-driven and state-feedback safety controllers, and transform constrained optimal control problems for CAVs into a sequence of event-triggered quadratic programs. We show that we can ensure collision-free interactions between HDVs and CAVs and demonstrate the robustness and flexibility of our framework on different types of human drivers in lane-changing scenarios while guaranteeing the satisfaction of safety constraints.**

I. INTRODUCTION

Connected and Automated Vehicles (CAVs), also known as "self-driving cars", promise to significantly transform the operation of transportation networks and improve their performance by assisting drivers in making decisions so as to reduce accidents, as well as travel times, energy consumption, air pollution, and traffic congestion [1]–[3]. The cooperative control of CAVs has attracted a surge of interest in providing opportunities for vehicles to travel safely and optimally while enhancing the efficient operation of traffic networks [4], [5].

However, 100% CAV penetration is not likely in the near future, raising the question of how to benefit from the presence of at least some CAVs in mixed traffic and to still guarantee safety when CAVs must interact with uncontrollable Human-Driven Vehicles (HDVs) [6]–[9]. To address this challenge, efforts have concentrated on developing accurate car-following models, as in [10], aiming at a deterministic quantification of HDV states, while [11] considers vehicle interactions, employs a prediction model to estimate HDV behaviors in real-time and directly controls CAVs to force HDVs to form platoons. In an effort to accurately model human driver behavior, a concept of social value orientation is defined in [12] to characterize an agent's proclivity for social behavior or individualism and further predict human behavior. Considering vehicle interactions, a game-theoretic approach is used in [13] to assist CAVs in evaluating the best possible response to an opponent's actions. While existing approaches have often shown impressive performance in managing vehicle interactions in mixed traffic, they assume known dynamics for HDVs. However, uncontrollable human behavior under real-world conditions makes HDV models difficult to rely on for accurate predictions, which further increases the collision risk for CAVs and compromises their ability to guarantee safety. Moreover, most of the methods used are computationally expensive. The high complexity of obtaining accurate solutions motivates the use of Control Barrier Functions (CBFs) [14], [15] to improve computation efficiency without compromising safety guarantees.

In recent years, CBFs have been frequently used to enforce system safety, and Control Lyapunov Functions (CLFs) are employed to make the system state converge to desired values, e.g., see [14], [16]–[20]. In general, constrained optimal control problems (with quadratic cost) can be solved by discretizing time and transforming them into a sequence of Quadratic Programs (QPs) at each time step with the assumption that control is a constant during each such time interval. This assumption gives rise to the problem that each time discretization interval needs to be sufficiently small to ensure the feasibility of each QP at any one time step. One way to solve this problem is to adopt *event-triggered* approaches as proposed in [21] and further in [22] to deal with unknown system dynamics. However, there has been little consideration of human factors in conjunction with CBFs.

In this paper, we study safe driving interactions between CAVs and HDVs in a mixed-traffic environment, in which case the dynamics and human control policies of HDVs are unknown. We adopt the event-triggered CBF method proposed in [22] for CAVs to ensure the safety between CAVs and HDVs, and implement it in highway lane-changing maneuvers. This work provides enhanced robustness of the optimal policies for uncontrollable HDVs in mixed traffic. The main contributions of this paper are summarized as follows

- We propose a safe and robust human interaction framework in mixed traffic using event-triggered CBFs under the case of unknown (generally nonlinear, but affine in the control) HDV dynamics and unpredictable human-in-the-loop control policies.
- Both longitudinal and lateral maneuvers are combined together in a lane-changing maneuver with an ellipsoidal safety region determined for vehicles so as to guarantee safety in a 2D manner during the entire maneuver.
- The optimal pair for the lane-changing CAV to merge in between is determined in real time, depending on the aggressiveness of HDVs.
- We demonstrate safe human interactions on different types of human drivers (e.g., aggressive, hesitant, con-

This work was supported in part by NSF under grants CNS-2149511, ECCS-1931600, DMS-1664644 and CNS-1645681, by ARPAE under grant DE-AR0001282, and by the MathWorks.

A. Li and C. G. Cassandras are with the Division of Systems Engineering and Center for Information and Systems Engineering, Boston University, Brookline, MA 02446. {anlianni, cgc}@bu.edu

W. Xiao is with the Computer Science and Artificial Intelligence Lab, Massachusetts Institute of Technology. weixy@mit.edu

servative) in mixed traffic highway lane merging.

II. PROBLEM FORMULATION

The highway lane-changing scenario is shown in Fig. 1, where the green vehicles 1 and C are assumed to be cooperating CAVs, the red vehicle H is an uncontrollable HDV, and the gray vehicle U is considered as a dynamic obstacle moving at a slower speed than CAVs. A lane-changing maneuver is triggered by C when an obstacle ahead is detected. In general, such a maneuver can be initiated at any arbitrary time set by C. The framework proposed in this paper can be used in any conflict area involving vehicle interactions, but we limit ourselves to this lane-changing setting which we view as the most challenging among them. We aim to minimize the maneuver time and energy expended, while alleviating any disruption to the fast lane traffic flow. Moreover, considering the presence of HDVs, C also needs to be aware of the behavior of its surrounding HDVs in order to guarantee safety.

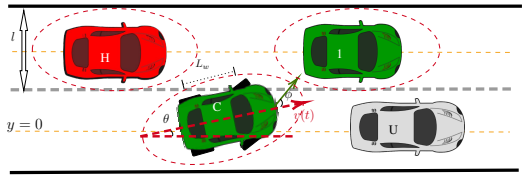

Fig. 1: The basic lane-changing maneuver process. The red vehicle is an HDV, green vehicles are CAVs, and the grey vehicle is a slow-moving and uncontrollable vehicle.

Vehicle Dynamics. The dynamics and control policy of the HDV are unknown in this case. Assume the slow vehicle U keeps traveling in the slow lane with a constant speed v_U. For each CAV in Fig. 1, indexed by $i \in \{1, C\}$, its dynamics take the form, as defined in [23]:

$$\underbrace{\begin{bmatrix} \dot{x}_i \\ \dot{y}_i \\ \dot{\theta}_i \\ \dot{v}_i \end{bmatrix}}_{\dot{\boldsymbol{x}}_i} = \underbrace{\begin{bmatrix} v_i \cos\theta_i \\ v_i \sin\theta_i \\ 0 \\ 0 \end{bmatrix}}_{f(\boldsymbol{x}_i(t))} + \underbrace{\begin{bmatrix} 0 & -v_i \sin\theta_i \\ 0 & v_i \cos\theta_i \\ 0 & v_i/L_w \\ 1 & 0 \end{bmatrix}}_{g(\boldsymbol{x}_i(t))} \underbrace{\begin{bmatrix} u_i \\ \phi_i \end{bmatrix}}_{\boldsymbol{u}_i(t)} \quad (1)$$

where $x_i(t), y_i(t), \theta_i(t), v_i(t)$ represent the current longitudinal position, lateral position, heading angle, and speed, respectively. $u_i(t)$ and $\phi_i(t)$ are the acceleration and steering angle (controls) of vehicle i at time t, respectively, $g(\boldsymbol{x}_i(t)) = [g_u(\boldsymbol{x}_i(t)), g_\phi(\boldsymbol{x}_i(t))]$. The maneuver starts at time t_0 and ends at time t_f when C has completely switched to the target lane. The control input and speed for all vehicles are constrained as follows:

$$\boldsymbol{u}_{i_{\min}} \le \boldsymbol{u}_i(t) \le \boldsymbol{u}_{i_{\max}}, v_{i_{\min}} \le v_i(t) \le v_{i_{\max}},\ i \in \{1, C\}, \quad (2)$$

where $\boldsymbol{u}_{i_{\min}}, \boldsymbol{u}_{i_{\max}} \in \mathbb{R}^2$ denote the minimum and maximum control bounds for vehicle i, respectively. $v_{i_{\min}} > 0$ and $v_{i_{\max}} > 0$ are vehicle i's allowable minimum and maximum speed. Setting l as the width of the road, $y = 0$ axis is the center of the slow lane in Fig. 1, we have $y_C(t_0) = 0$, and the lateral positions of vehicles satisfy

$$-\frac{l}{2} \le y_i(t) \le \frac{3}{2}l,\ i \in \{1, C\}. \quad (3)$$

Safety Constraints. Similar to the longitudinal safe distance described in [15], we define an ellipsoidal safe region $b_{i,j}(\boldsymbol{x}_i, \boldsymbol{x}_j)$ for vehicles i and j during the entire maneuver:

$$b_{i,j} := \frac{(x_j(t) - x_i(t))^2}{(a_i v_i(t))^2} + \frac{(y_j(t) - y_i(t))^2}{(b_i v_i(t))^2} - 1 \ge 0, \quad (4)$$

where j is i's neighboring vehicle, a_i, b_i are weights adjusting the length of the major and minor axes of the ellipse, and the size of the safe region depends on speed. Note that $b_{i,j}$ is specified from the center of vehicle i to the center of j. Defining an elliptical safe region considers the 2D safe distance between two vehicles. Since (4) depends on speed, its CBF constraint only has relative degree one, implying lower complexity in CBF design.

Remark 1: Other than the elliptical format, a circle or multiple disks can also be adopted to describe the safe region between vehicles as long as the equation is differentiable with respect to time and system states.

Optimal Control Problem Formulation. Our goal is to determine the optimal control policy for CAV C to perform a safe lane change maneuver. The objective is to jointly minimize C's energy consumption and speed deviation from traffic flow while guaranteeing safety. Considering cooperations between C and 1, the joint cooperative optimal control problem (OCP) for both CAVs is given by:

$$\min_{u_C(t), u_1(t), t_f} \int_{t_0}^{t_f} \frac{\alpha_u}{2}(u_C^2(t) + u_1^2(t))dt + \alpha_l(y_C(t_f) - l)^2 + \alpha_v[(v_C(t_f) - v_d)^2 + (v_1(t_f) - v_d)^2] \quad (5)$$
$$s.t.\ \ (1),\ (2),\ (3),\ (4)$$

where v_d denotes the desired speed of CAVs in the fast lane, $\alpha_u, \alpha_l, \alpha_v$ are adjustable non-negative (properly normalized) weights for energy, desired lateral position, and desired speed, respectively. The CAV dynamics are given in (1) with state and control limits as in (2) and (3). Safety distances between all vehicle pairs in Fig. 1 are constrained through (4), requiring state knowledge of all vehicles. However, since HDVs are uncontrollable and unknown to CAVs in actuality, coupling the unknown HDV states with CAVs in the safety constraint between C and H makes (5) directly unsolvable.

Therefore, in this paper, we employ event-triggered CBFs [22] to solve (5). The CBF method replaces the safety constraints in the OCP with new CBF-based constraints which are linear in the control and imply the original constraints. In particular, for any state constraint $b(x)$, the general form of the associated CBF constraint is (see [15]):

$$\sup_{\boldsymbol{u} \in \mathcal{U}} [L_f b(\boldsymbol{x}) + L_g b(\boldsymbol{x}) \boldsymbol{u} + \alpha(b(\boldsymbol{x}))] \ge 0,\ \forall x \in C, \quad (6)$$

where L_f, L_g denote the Lie derivatives of $b(x)$ along f and g, respectively. It is assumed that $L_g b(\boldsymbol{x}) \neq 0$ when $b(\boldsymbol{x}) = 0$. The critical step to solve OCP (5) using event-triggered CBFs is to first estimate HDV dynamics, then, at each time step, CAVs can proceed with their maneuvers based on HDV state estimates, and replace the safety constraints with the CBF constraints to enforce their satisfaction. Then, the problem (5) can be transformed into a sequence of QPs similar to

[14]. Finally, we implement an *event-driven* approach in the CBF-based QPs to find the next triggering time to solve the QP. The details of the overall framework are described in the following section.

III. HUMAN-IN-THE-LOOP SAFE LANE-CHANGING MANEUVER

A. CBFs with Adaptive Dynamics for HDVs

In this section, we introduce adaptive dynamics for the HDV based on real-time measurements so as to approximate its actual dynamics. We begin by assuming adaptive nonlinear dynamics for the HDV:

$$\dot{\bar{\boldsymbol{x}}}_H = f_a(\bar{\boldsymbol{x}}_H) + g_a(\bar{\boldsymbol{x}}_H)\boldsymbol{u}_H, \tag{7}$$

where $f_a : \mathbb{R}^n \to \mathbb{R}$, $g_a : \mathbb{R}^n \to \mathbb{R}^{n\times q}$ are adaptive functions to accommodate the real unknown HDV dynamics, $u_H \in \mathbb{R}^q$ is the control input of HDV, and $\bar{\boldsymbol{x}}_H \in X \subset \mathbb{R}^n$ is the estimated state vector corresponding to the real HDV states $\boldsymbol{x}_H$. Let $\boldsymbol{e} := \boldsymbol{x}_H - \bar{\boldsymbol{x}}_H$ be the direct measurement error between the real HDV states $\boldsymbol{x}_H$ and estimated states $\bar{\boldsymbol{x}}_H$. Then for any safety function $b_{i,H}(\boldsymbol{x}_i, \boldsymbol{x}_H)$ defined in (4) between vehicles i and H, it has to satisfy

$$b_{i,H}(\boldsymbol{x}_i, \boldsymbol{x}_H) = b_{i,H}(\boldsymbol{x}_i, \bar{\boldsymbol{x}}_H + \boldsymbol{e}) \geq 0. \tag{8}$$

Equivalent to the CBF constraint defined in (6), we have the CBF constraint to enforce safety for the unknown-dynamics HDV in the form

$$\begin{aligned}&\frac{\partial b_{i,H}(\boldsymbol{x}_i, \bar{\boldsymbol{x}}_H + \boldsymbol{e})}{\partial \boldsymbol{x}_i}\dot{\boldsymbol{x}}_i + \frac{\partial b_{i,H}(\boldsymbol{x}_i, \bar{\boldsymbol{x}}_H + \boldsymbol{e})}{\partial \bar{\boldsymbol{x}}_H}\dot{\bar{\boldsymbol{x}}}_H \\ &+ \frac{\partial b_{i,H}(\boldsymbol{x}_i, \bar{\boldsymbol{x}}_H + \boldsymbol{e})}{\partial \boldsymbol{e}}\dot{\boldsymbol{e}} + \alpha(b_{i,H}(\boldsymbol{x}_i, \bar{\boldsymbol{x}}_H + \boldsymbol{e})) \geq 0.\end{aligned} \tag{9}$$

where $\dot{\boldsymbol{x}}_i, \dot{\bar{\boldsymbol{x}}}_H$ are described by dynamics (1) and (7), respectively, and $b_{i,H}(\boldsymbol{x}_i, \bar{\boldsymbol{x}}_H + \boldsymbol{e})$ is given by (4). The only unknown terms left in (9) are $\boldsymbol{e}$ and $\dot{\boldsymbol{e}}$, which can be evaluated by direct measurements online. Therefore, the satisfaction of (9) implies the satisfaction of safety constraint $b_{i,H}(\boldsymbol{x}_i, \boldsymbol{x}_H) \geq 0$ even if the dynamics of $\boldsymbol{x}_H$ is unknown to CAVs, as shown in [22]. Then, we transform (5) into a sequence of QPs, and update $f_a(\bar{\boldsymbol{x}}_H)$ of the adaptive dynamics (7) at each time step $t_k, k = 1, 2, ...$ with

$$f_a(\bar{\boldsymbol{x}}(t_k^+)) = f_a(\bar{\boldsymbol{x}}(t_k^-)) + \dot{\boldsymbol{e}}(t_k), \tag{10}$$

where t_k^+, t_k^- denote the instants right after and before t_k. In this way, we always have the measurements such that $\boldsymbol{e}(t_k) = \boldsymbol{0}$ and $\dot{\boldsymbol{e}}(t_k^+)$ close to 0 at t_k by setting $\bar{\boldsymbol{x}}_H(t_k) = \boldsymbol{x}_H(t_k)$. This reduces the number of events (introduced later) to solve the QP and reduce the conservativeness of CAVs.

B. Transform OCP to CBF-based QPs

In a lane-changing maneuver, we define adaptively updated dynamics for the HDV traveling in the fast lane in the form:

$$\underbrace{\begin{bmatrix}\dot{\bar{x}}_H \\ \dot{\bar{y}}_H \\ \dot{\bar{\theta}}_H \\ \dot{\bar{v}}_H\end{bmatrix}}_{\dot{\bar{\boldsymbol{x}}}_H(t)} = \underbrace{\begin{bmatrix}\bar{v}_H \cos\bar{\theta}_H + h_x(t) \\ \bar{v}_H \sin\bar{\theta}_H + h_y(t) \\ \bar{v}_H/L_w + h_\theta(t) \\ h_v(t)\end{bmatrix}}_{f_a(\bar{\boldsymbol{x}}_H(t))} \tag{11}$$

where $\bar{\boldsymbol{x}}_H = [\bar{x}_H(t), \bar{y}_H(t), \bar{\theta}_H(t), \bar{v}_H(t)]^T$ represent the estimated longitudinal position, lateral position, heading angle, and speed of the HDV, respectively. Note that $h_{x,y,\theta,v}(t) \in \mathbb{R}^n$ denote the adaptive terms to approximate the real HDV dynamics, where we set $h_j(t_0) = 0$ for all $j \in \{x, y, \theta, v\}$.

Derive CBF Constraints: Firstly, we derive the CBF constraints to make sure the speed and control constraint (2), position constraint (3), and safety constraints (4) in OCP (5) are satisfied at all times. Each of the constraints above can be written in the form $b_n(\boldsymbol{x})$, $n \in \{1, 2, ..., N\}, \boldsymbol{x} = \{\boldsymbol{x}_1, \boldsymbol{x}_C, \boldsymbol{x}_H, \boldsymbol{x}_U\}$, where N is the number of constraints, and we can always apply the CBF method to map a constraint $b_n(\boldsymbol{x})$ to a new CBF constraint for vehicles $i \in \{1, C, H, U\}$ by using the general expression (6)

$$L_f b_n(\boldsymbol{x}) + L_g b_n(\boldsymbol{x})\boldsymbol{u} + \alpha_n(b_n(\boldsymbol{x})) \geq 0, \tag{12}$$

with $\boldsymbol{u} = \{\boldsymbol{u}_1, \boldsymbol{u}_C\}$. We omit further details here.

Derive CLF Constraints: In addition to CBFs used for hard constraints, we use Control Lyapunov Functions (CLFs) (see [14]) associated with the terminal costs in (5) to achieve lane-keeping and to minimize speed deviations from the desired speed v_d for CAVs. Setting $V_1(\boldsymbol{x}_C(t)) = (v_C(t) - v_d)^2$, $V_2(\boldsymbol{x}_1(t)) = (v_1(t) - v_d)^2$, $V_3(\boldsymbol{x}_C(t)) = (y_C(t) - l)^2$, and $V_4(\boldsymbol{x}_1(t)) = (y_1(t) - l)^2$, the CLF constraints can be calculated accordingly based on the general expression:

$$L_f V(\boldsymbol{x}) + L_g V(\boldsymbol{x})\boldsymbol{u} + c_3 V(\boldsymbol{x}) \leq \delta, \tag{13}$$

where δ is denoted as the controllable variable to treat (13) as a soft constraint.

Time Discretization: Finally, we discretize time and let t_k, $k = 1, 2, ...$ be the time instants when C solves the QPs. A common way is to adopt the *time-driven* approach and select a fixed length Δ for each time interval such that $t_k = t_0 + k\Delta$. The OCP (5) can be transformed into a sequence of QPs (each solved at the kth time step) as follows:

$$\min_{u_i(t_k), \delta_j(t_k)} \sum_{i=1,C} \alpha_{u_i} u_i^2(t_k) + \sum_{j=1}^{4} p_j \delta_j^2(t_k) \tag{14}$$

subject to CBF constraints (12) corresponding to constraints (2), (3), (4), and CLF constraints (13) corresponding to the Lyapunov function $V_j(\boldsymbol{x}), j \in \{1, 2, 3, 4\}$. The weights $\alpha_{u_i}, i \in \{1, C\}$ and $p_j, j \in \{1, 2, 3, 4\}$ are adjustable, used to provide a relative importance to each corresponding term in the objective function.

C. Event-driven Control

Following the time-driven approach to solving (14) at each time step $t_k, k = 1, 2, ...$, we cannot guarantee the satisfaction of CBF constraints because the state error $\boldsymbol{e}$ and its derivative $\dot{\boldsymbol{e}}$ are generally unknown to the solver right after t_k. As introduced in [22], the key idea of the event-driven approach is to properly define events depending on state errors and their derivatives so that the QPs will be solved at each event-triggered time t_k while the safety CBF constraints remain satisfied during the time interval $[t_k, t_{k+1})$.

Set Bounds for Error: In order to find a condition to guarantee the satisfaction of CBF constraints for $t \in$

$[t_k, t_{k+1})$, we first assume that the state error and its derivative satisfy

$$|e_x| \leq w_x, \quad |e_y| \leq w_y, \quad |e_\theta| \leq w_\theta, \quad |e_v| \leq w_v, \tag{15a}$$

$$|\dot{e}_x| \leq \nu_x, \quad |\dot{e}_y| \leq \nu_y, \quad |\dot{e}_\theta| \leq \nu_\theta, \quad |\dot{e}_v| \leq \nu_v, \tag{15b}$$

where $\boldsymbol{w} := [w_x, w_y, w_\theta, w_v]^T \in \mathbb{R}^4_{\geq 0}$, and $\boldsymbol{\nu} := [\nu_x, \nu_y, \nu_\theta, \nu_v]^T \in \mathbb{R}^4_{\geq 0}$ are chosen bounds that determine the conservativeness of the framework. Specifically, small bounds introduce less conservativeness with more events, and vice versa. Similarly, we consider the state vector $\boldsymbol{x}_i$ for all vehicles $i \in \{1, C, H, U\}$ at time t_k, which satisfies the following bounds $\boldsymbol{x}_i(t_k) - \boldsymbol{s}_i \leq \boldsymbol{x}_i(t) \leq \boldsymbol{x}_i(t_k) + \boldsymbol{s}_i$, where $\boldsymbol{s}_i \in \mathbb{R}^4_{\geq 0}$ is a parameter vector similar to error bounds. We denote a set for states of vehicle i at time t_k as

$$S_i(t_k) = \{\boldsymbol{z}_i \in X : \boldsymbol{x}_i(t_k) - \boldsymbol{s}_i \leq \boldsymbol{z}_i \leq \boldsymbol{x}_i(t_k) + \boldsymbol{s}_i\} \tag{16}$$

Besides, we define a feasible set $C_{i,1}$ for vehicle $i \in \{1, C, H, U\}$ as $C_{i,1} := \{\boldsymbol{x}_i \in X : b_n(\boldsymbol{x}) \geq 0, \ n \in 1, 2, ..., N\}$ such that all original constraints (1), (2), (3), (4) are satisfied: Based on these settings, we can proceed to find a condition that guarantees the satisfaction of all CBF constraints in the time interval $[t_k, t_{k+1})$, which can be done by minimizing each component in (12). We take the CBF constraint between vehicles C and H as an example to illustrate the detailed process.

Find Robust CBFs: In (12), assume $\alpha(\cdot)$ is linear with scalar $k_{i,j}$ for each constraint $b_{i,j}$. Let $L_{f_{\min}} b_{C,H}(t_k) \in \mathbb{R}$ be the minimum value of $L_f b_{C,H}(\boldsymbol{x}_C, \boldsymbol{x}_H) + k_{C,H} b_{C,H}(\boldsymbol{x}_C, \boldsymbol{x}_H)$ for the proceeding time interval that satisfies $\boldsymbol{r} \in R(t_k)$ where $\boldsymbol{r} := [\boldsymbol{z}_C, \boldsymbol{z}_H, \boldsymbol{e}, \dot{\boldsymbol{e}}]^T, R(t_k) := \{\boldsymbol{r} : \boldsymbol{z}_C \in S_C(t_k), \boldsymbol{z}_H \in S_H(t_k), |\boldsymbol{e}| \leq \boldsymbol{w}, |\dot{\boldsymbol{e}}| \leq \boldsymbol{\nu}, \boldsymbol{z}_H + \boldsymbol{e} \in C_{H,1}\}$, at time t_k:

$$L_{f_{\min}} b_{C,H}(t_k) = \min_{\boldsymbol{r} \in R(t_k)} L_f b_{C,H}(\boldsymbol{z}_C, \boldsymbol{z}_H) + k_{C,H} b_{C,H}(\boldsymbol{z}_C, \boldsymbol{z}_H) \tag{17}$$

The remaining term $L_g b_{C,H}(\boldsymbol{x}_C, \boldsymbol{x}_H)\boldsymbol{u}_C$ in (12) contains the control input $\boldsymbol{u}_C = [u_C, \phi_C]^T$, which complicates the minimization process. To minimize this term, we need to consider the sign of ϕ_C, u_C at time t_k. Similar to (17), set

$$L_{g_{\min}} b_{C,H}(t_k) = [L_{g_u \min} b_{C,H}(t_k), L_{g_\phi \min} b_{C,H}(t_k)]$$

as the vector of minimum values of $L_g b_{C,H}(\boldsymbol{x}_C, \boldsymbol{x}_H)$ for the proceeding time interval. Then, we have

$$L_{g_\phi \min} b_{C,H}(t_k) = \begin{cases} \min\limits_{\boldsymbol{r} \in R(t_k)} L_{g_\phi} b_{C,H}(\boldsymbol{z}_C, \boldsymbol{z}_H), & if \ \phi_C(t_k) \geq 0, \\ \max\limits_{\boldsymbol{r} \in R(t_k)} L_{g_\phi} b_{C,H}(\boldsymbol{z}_C, \boldsymbol{z}_H), & otherwise. \end{cases} \tag{18}$$

and

$$L_{g_u \min} b_{C,H}(t_k) = \begin{cases} \min\limits_{\boldsymbol{r} \in R(t_k)} L_{g_u} b_{C,H}(\boldsymbol{z}_C, \boldsymbol{z}_H), & if \ u_C(t_k) \geq 0, \\ \max\limits_{\boldsymbol{r} \in R(t_k)} L_{g_u} b_{C,H}(\boldsymbol{z}_C, \boldsymbol{z}_H), & otherwise. \end{cases} \tag{19}$$

where the sign of ϕ_C, u_C can be obtained by simply solving (14) at time t_k. Therefore, the condition that guarantees the satisfaction of (12) during $[t_k, t_{k+1})$ is given by

$$L_{f_{\min}} b_{C,H}(t_k) + L_{g_{\min}} b_{C,H}(t_k)\boldsymbol{u}_C \geq 0. \tag{20}$$

Similarly, for all CBF constraints with the form (12), they have to satisfy the condition

$$L_{f_{\min}} b_n(t_k) + L_{g_{\min}} b_n(t_k)\boldsymbol{u} \geq 0, \tag{21}$$

where $L_{f_{\min}} b_n(t_k)$ is the minimum value of $L_f b_n(\boldsymbol{x}) + \alpha_n(b_n(\boldsymbol{x}))$, and $L_{g_{\min}} b_n(t_k)\boldsymbol{u}$ is the minimum value of $L_g b_n(\boldsymbol{x})\boldsymbol{u}$ during $[t_k, t_{k+1})$.

In order to apply the above conditions to the QP (14), we just replace all the CBF constraints (12) by (21), i.e.,

$$\min_{u_i(t_k), \delta_j(t_k)} \sum_{i=1,C} \alpha_{u_i} u_i^2(t_k) + \sum_{j=1}^{4} p_j \delta_j^2(t_k) \tag{22}$$

subject to the CAV dynamics (1), CBF conditions (21), and CLF constraints (13) corresponding to $V_j(\boldsymbol{x}), j \in \{1, 2, 3, 4\}$.

Determine Triggering Events: Based on the above settings, we define three events that specify the conditions for triggering an instance of solving QP (22):

Event 1: The measured HDV state error $\boldsymbol{e}$ exceeds its bounds $\boldsymbol{w}$, i.e., any one inequality in (15a) is about to be violated.

Event 2: The measured derivative of the HDV state error $\dot{\boldsymbol{e}}$ exceeds its bounds $\boldsymbol{\nu}$, i.e., any one inequality in (15b) is about to be violated.

Event 3: The state measurement of vehicle $i, i \in \{1, C, H, U\}$ reaches the boundaries of $S_i(t_k)$.

The first two events can be detected by directly measuring the state error and its derivative, and the third event is detected by monitoring the dynamics of (1) and (11). Therefore, the next event-triggered time $t_{k+1}, k = 0, 1, 2, ...$ is given by

$$t_{k+1} = \min\{t > t_k : |\boldsymbol{e}| = \boldsymbol{w} \text{ or } |\dot{\boldsymbol{e}}| = \boldsymbol{\nu} \text{ or } |\boldsymbol{x}_i(t) - \boldsymbol{x}_i(t_k)| = \boldsymbol{s}_i \text{ or } |\bar{\boldsymbol{x}}_H(t) - \bar{\boldsymbol{x}}_H(t_k)| = \boldsymbol{s}_H\}, \tag{23}$$

where $i \in \{1, C, U\}$ in (23). Recalling that the real HDV dynamics are unknown, we apply its estimated states $\bar{\boldsymbol{x}}_H$ from (11) to check the next triggered time t_{k+1}. The choice of each component of $\boldsymbol{s}_i$ in (16) captures the tradeoff between the time complexity and the conservativeness of the approach.

In summary, to solve OCP (5), the first step is to estimate HDV dynamics at each time step t_k and transform the problem into a series of QPs. Then, at each t_k, CAVs can proceed with their maneuvers based on HDV state estimates, and replace the safety constraints with the event-triggered CBF constraints to enforce their satisfaction. Finally, we implement an *event-driven* control to find the next triggering time. The details of the overall framework are described in [24].

IV. SIMULATION RESULTS

This section provides simulation results illustrating the optimal lane-changing trajectories for each CAV with safety guarantees in mixed traffic, even though the HDV dynamics are unknown to CAVs. We emphasize that the controller can be implemented to monitor the HDV's behavior and respond to HDVs in real-time. We test our framework by allowing human drivers to manually operate virtual vehicles through a MATLAB interface, and the results show that CAV C can always update its control to avoid collisions and successfully perform a safe maneuver. Our simulation

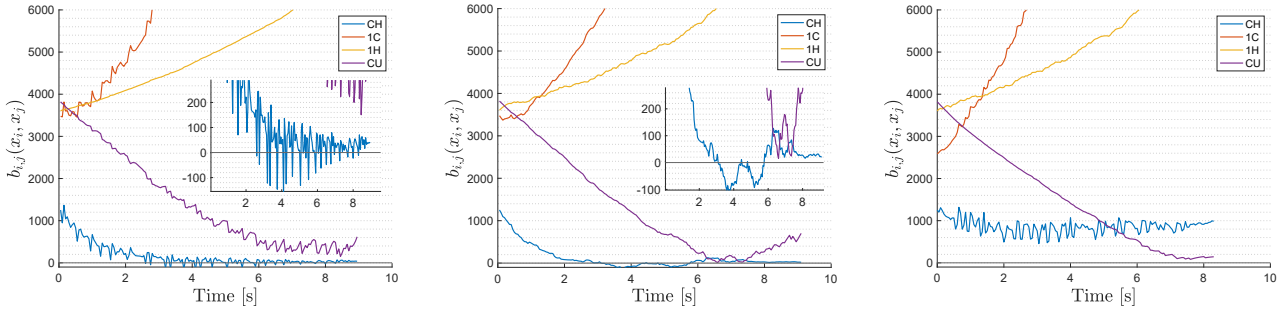

(a) Case 1: Time-driven approach with known HDV dynamics

(b) Case 2: Time-driven approach with unknown HDV dynamics

(c) Case 3: Event-driven approach with unknown HDV dynamics

Fig. 2: Safety with time-driven and event-driven CBFs. $b_{i,j}(\boldsymbol{x}_i, \boldsymbol{x}_j)$ denotes the value of the CBF between vehicles i and j, where $(i,j) \in \{(C,H),(1,C),(1,H),(C,U)\}$. $b_{i,j}(\boldsymbol{x}_i, \boldsymbol{x}_j) \geq 0$ denotes safety guarantees (Case 3, not Cases 1 and 2).

setting is that of Fig. 1. Vehicle U is assumed to travel with constant speed $v_U = 20\ m/s$ all the time (this is not needed in the overall approach). The dynamics of vehicle C and 1 are followed by (1). The allowable speed range for CAVs is $v \in [15, 35] m/s$, and the acceleration of vehicles is limited to $\boldsymbol{u} \in [(-7, -\pi/4), (3.3, \pi/4)] m/s^2$. The desired speed v_d for the CAVs is considered as the traffic flow speed, which is set to 30 m/s. To guarantee safety, in designing the size of the ellipse in (4) as a safe region, we set the parameters $a_C = a_1 = 0.6$ as the reaction time of CAVs, and $b_1 = b_C = 0.1$ to let the minor axis approximate the lane width $l = 4\ m$. The maximum allowable maneuver time is set at $T_f = 15\ s$. The real HDV dynamics are **unknown** to the controller and expressed as:

$$\begin{bmatrix} \dot{x}_H \\ \dot{y}_H \\ \dot{\theta}_H \\ \dot{v}_H \end{bmatrix} = \begin{bmatrix} v_H \cos\theta_H \cdot \sigma_1 \\ v_H \sin\theta_H \cdot \sigma_2 \\ 0 \\ 0 \end{bmatrix} + \begin{bmatrix} 0 & -v_H \sin\theta_H \\ 0 & v_H \cos\theta_H \\ 0 & v_H / L_w \\ 1 & 0 \end{bmatrix} \begin{bmatrix} u_H \\ \phi_H \end{bmatrix} + \begin{bmatrix} \varepsilon_1 \\ \varepsilon_2 \\ \varepsilon_3 \\ \varepsilon_4 \end{bmatrix} \tag{24}$$

where $\boldsymbol{u}_H$ is either a random policy or controlled by a human player. σ_1, σ_2 denote two random processes with uniform pdfs over the interval $[0.9, 1.1]$, and $\varepsilon_1 \in [-0.7, 0.7], \varepsilon_2 \in [-0.5, 0.5], \varepsilon_3 \in [-0.5, 0.5], \varepsilon_4 \in [-0.7, 0.7]$ are disturbances. The initial states of vehicles at time $t_0 = 0$ are given as $\boldsymbol{x}_C(t_0) = [20\ m, 0\ m, 0\ rad, 25\ m/s]^T$, $\boldsymbol{x}_1(t_0) = [50\ m, 4\ m, 0\ rad, 29\ m/s]^T$, $\boldsymbol{x}_H(t_0) = [10\ m, 4\ m, 0\ rad, 28\ m/s]^T, \boldsymbol{x}_U(t_0) = [60\ m, 0\ m, 0\ rad, 20\ m/s]^T$. The weights in QP (22) are set as $\alpha_{u_1} = \alpha_{u_C} = 1$, $p_1 = p_2 = p_4 = 1, p_3 = 100$. The initial states of the adaptive HDV dynamics (11) are set as $\bar{\boldsymbol{x}}_H(t_0) = \boldsymbol{x}_H(t_0)$, and the adaptive terms at t_0 satisfy $h_x(t_0) = h_y(t_0) = h_\theta(t_0) = h_v(t_0) = 0$.

The parameters $\boldsymbol{s}_i$ in the feasible set S_i are $\boldsymbol{s}_i = [0.01\ m, 0.005\ m, 0.01\ rad, 1\ m/s]$ for all vehicles $i \in \{1, C, H, U\}$. The bound for state error $\boldsymbol{e}$ and its derivative $\dot{\boldsymbol{e}}$ are given as $\boldsymbol{w} = [0.2\ m, 0.1\ m, 0.1\ rad, 1\ m/s]$, $\boldsymbol{\nu} = [0.5\ m/s, 0.2\ m/s, 0.1\ rad/s, 1\ m/s^2]$. The allowable error to terminate the maneuver is $\epsilon = 0.3\ m$. The numerical solutions to the QPs are obtained using an interior point optimizer (IPOPT) on an Intel(R) Core(TM) i7-8700 3.20GHz. The computation times for time-driven and event-driven approaches are $1.5\ ms$ and $24.0\ ms$, respectively.

A. Comparison between Time and Event Driven Approach

Based on the above settings, we compare our event-triggered approach in solving CBF-based QPs (22) with unknown HDV dynamics to a time-driven approach. Set the discretized time interval $\Delta = 0.05\ s$. Due to inter-sampling effects on system performance when applying a time-driven approach, we consider three cases to test the effectiveness of the event-driven approach in implementing the lane-changing problem. The HDV policy is set to be random, satisfying $u_H(t_k) \in [-1.7, 1.7] m/s^2, \phi_H(t_k) \in [-0.2\pi, 0.2\pi] rad, k = 0, 1, 2, ...$

Case 1: Time-driven approach with known HDV dynamics.
Case 2: Time-driven approach with unknown HDV dynamics.
Case 3: Event-driven approach with unknown HDV dynamics.

The simulation results are shown in Fig. 2, where the x-axis denotes the simulation time and the y-axis denotes the value of safety constraint $b_{i,j}$ in (4). $b_{i,j} < 0$ represents a violation of the safety constraint between vehicles i and j. In Fig. 2, the distances between vehicles 1 and C (red curve), vehicles 1 and H (yellow curve) keep increasing. The two constraints about to be violated are $b_{C,U}$ (purple curve) and $b_{C,H}$ (blue curve). From Fig. 2a, even if the HDV dynamics are assumed to be known to CAV C, we still have $b_{C,H} < 0$ at some points, which means the distance between vehicles C and H is less than the safe distance. Similar results occur in Fig. 2b, where $b_{C,H}$ (blue curve) is below 0 at some points, violating safety during the maneuver. Safety is not guaranteed even with state synchronization under the time-driven approach. In Fig. 2c, all curves are above 0, implying safety guarantees for all vehicles during the lane-changing maneuver.

B. Human Driver Case Studies

In this section, we further introduce human control in the framework through which the human driver's aggressiveness will affect CAV responses. We have drivers perform *aggressive, hesitant, and conservative* driving behaviors to test the proposed approach through the merging point, safety satisfaction, maneuver time, and energy consumption. The simulation results for three types of driving players are summarized in Table. I. Given the safety constraint that is about to be violated is $b_{C,H}$ between vehicles C and H (from the results in Fig. 2), the column "Safety" in Table. I

Human Driver Type	Times		Safety	Terminal Time $t_f[s]$	Energy
	A-HDV	B-HDV			
Aggressive	0	10	627.7	3.4±0.3	27.1±25.9
Hesitant	5	5	521.2	8.8±1.4	63.2±46.2
Conservative	10	0	575.6	3.8±0.7	18.8±17.0

TABLE I: Performance of CAV C under different human driver types. "A-HDV" and "B-HDV" represent merging ahead of HDV and behind HDV, respectively. "Safety" denotes the minimum value of $b_{C,H}$ during the entire maneuver in the repeated 10 times.

is defined as the minimum value of $b_{C,H}(t_k), k = 0, 1, 2, ...$ during the entire maneuver.

Table I shows that if the human driver is aggressive, C is always conservative and chooses to merge behind the HDV. On the contrary, if the human driver is conservative, then it is safe for C to behave aggressively and merge ahead of the HDV. If the human driver is hesitant, the merging point varies and depends on the real-time traffic conditions. Note that all values in the Safety column are positive, which indicates no safety constraint is ever violated under the proposed event-driven approach. Moreover, considering the maneuver time t_f in view of energy consumption, we notice that when the driver's intention is explicit, i.e., the human driver is aggressive or conservative, C can respond and merge quickly by adapting to the HDV's behavior: the average maneuver time is $3.4\ s$ and $3.8\ s$, respectively, with corresponding energy consumptions 27.1 and 18.8. However, if the human driver performs hesitantly, the driver intention is not clear to CAV C, so that it always travels in a conservative manner with a longer average maneuver time of $8.8\ s$, and higher energy consumption of 63.2. This motivates exploring an optimal way to evaluate human characteristics in advance so that C can make decisions earlier, hence improving its performance. The videos for three types of drivers (human players) can be found in https://drive.google.com/drive/folders/1JQQ0mRMX35bEV6wsbPHmoM6UdOLMW2Dv?usp=sharing.

V. CONCLUSIONS

This paper proposes a robust framework for safe human interactions in mixed traffic, in which case the connected and automated vehicles can always guarantee safety with respect to human driven vehicles. This framework is mainly based on the real-time estimation of the human driven vehicle dynamics and control policy and the incorporation of such estimations into the event-triggered control barrier functions. Simulation results in mixed traffic highway merging with different types of human drivers have demonstrated the effectiveness and robustness of the proposed framework in guaranteeing the safety of all the vehicles. Future work will focus on estimating the characteristics of human drivers and seeking more efficient performance for CAV maneuvers.

REFERENCES

[1] J. Guanetti, Y. Kim, and F. Borrelli, "Control of connected and automated vehicles: State of the art and future challenges," *Annual reviews in control*, vol. 45, pp. 18–40, 2018.

[2] D. Schrank, B. Eisele, T. Lomax, and J. Bak, "Urban mobility scorecard," *Texas A&M Transportation Institute*, vol. 39, p. 5, 2015.

[3] M. Tideman, M. C. van der Voort, B. van Arem, and F. Tillema, "A review of lateral driver support systems," in *2007 IEEE Intelligent Transportation Systems Conference*. IEEE, 2007, pp. 992–999.

[4] J. Rios-Torres and A. A. Malikopoulos, "A survey on the coordination of connected and automated vehicles at intersections and merging at highway on-ramps," *IEEE Transactions on Intelligent Transportation Systems*, vol. 18, no. 5, pp. 1066–1077, 2016.

[5] H. Xu, S. Feng, Y. Zhang, and L. Li, "A grouping-based cooperative driving strategy for cavs merging problems," *IEEE Transactions on Vehicular Technology*, vol. 68, no. 6, pp. 6125–6136, 2019.

[6] A. Ghiasi, X. Li, and J. Ma, "A mixed traffic speed harmonization model with connected autonomous vehicles," *Transportation Research Part C: Emerging Technologies*, vol. 104, pp. 210–233, 2019.

[7] J. Wang, Y. Zheng, Q. Xu, J. Wang, and K. Li, "Controllability analysis and optimal control of mixed traffic flow with human-driven and autonomous vehicles," *IEEE Transactions on Intelligent Transportation Systems*, vol. 22, no. 12, pp. 7445–7459, 2020.

[8] A. S. C. Armijos, A. Li, C. G. Cassandras, Y. K. Al-Nadawi, H. Araki, B. Chalaki, E. Moradi-Pari, H. N. Mahjoub, and V. Tadiparthi, "Cooperative energy and time-optimal lane change maneuvers with minimal highway traffic disruption," *Automatica (to appear)*, 2024, (arXiv:2211.08636).

[9] A. Li, A. S. C. Armijos, and C. G. Cassandras, "Cooperative lane changing in mixed traffic can be robust to human driver behavior," *62nd IEEE Conf. on Decision and Control*, 2023.

[10] L. Zhao, A. Malikopoulos, and J. Rios-Torres, "Optimal control of connected and automated vehicles at roundabouts: An investigation in a mixed-traffic environment," *IFAC-PapersOnLine*, vol. 51, no. 9, pp. 73–78, 2018.

[11] A. I. Mahbub, V.-A. Le, and A. A. Malikopoulos, "A safety-prioritized receding horizon control framework for platoon formation in a mixed traffic environment," *Automatica*, vol. 155, p. 111115, 2023.

[12] W. Schwarting, A. Pierson, J. Alonso-Mora, S. Karaman, and D. Rus, "Social behavior for autonomous vehicles," *Proceedings of the National Academy of Sciences*, vol. 116, no. 50, pp. 24 972–24 978, 2019.

[13] M. Wang, Z. Wang, J. Talbot, J. C. Gerdes, and M. Schwager, "Game theoretic planning for self-driving cars in competitive scenarios." in *Robotics: Science and Systems*, 2019.

[14] A. D. Ames, J. W. Grizzle, and P. Tabuada, "Control barrier function based quadratic programs with application to adaptive cruise control," in *53rd IEEE Conference on Decision and Control*. IEEE, 2014, pp. 6271–6278.

[15] W. Xiao, C. G. Cassandras, and C. Belta, *Safe Autonomy with Control Barrier Functions: Theory and Applications*. Springer Nature, 2023.

[16] A. D. Ames, K. Galloway, and J. W. Grizzle, "Control lyapunov functions and hybrid zero dynamics," in *2012 IEEE 51st IEEE Conference on Decision and Control (CDC)*. IEEE, 2012, pp. 6837–6842.

[17] L. Wang, A. D. Ames, and M. Egerstedt, "Safety barrier certificates for collisions-free multirobot systems," *IEEE Transactions on Robotics*, vol. 33, no. 3, pp. 661–674, 2017.

[18] B. T. Lopez, J.-J. E. Slotine, and J. P. How, "Robust adaptive control barrier functions: An adaptive and data-driven approach to safety," *IEEE Control Systems Letters*, vol. 5, no. 3, pp. 1031–1036, 2020.

[19] W. Xiao, C. G. Cassandras, and C. A. Belta, "Bridging the gap between optimal trajectory planning and safety-critical control with applications to autonomous vehicles," *Automatica*, vol. 129, p. 109592, 2021.

[20] E. Sabouni, H. S. Ahmad, W. Xiao, C. G. Cassandras, and W. Li, "Optimal control of connected automated vehicles with event-triggered control barrier functions: a test bed for safe optimal merging," in *2023 IEEE Conference on Control Technology and Applications (CCTA)*. IEEE, 2023, pp. 321–326.

[21] P. Tabuada, "Event-triggered real-time scheduling of stabilizing control tasks," *IEEE Transactions on Automatic control*, vol. 52, no. 9, pp. 1680–1685, 2007.

[22] W. Xiao, C. Belta, and C. G. Cassandras, "Event-triggered control for safety-critical systems with unknown dynamics," *IEEE Transactions on Automatic Control*, vol. 68, no. 7, pp. 4143–4158, 2023.

[23] S. He, J. Zeng, B. Zhang, and K. Sreenath, "Rule-based safety-critical control design using control barrier functions with application to autonomous lane change," in *2021 American Control Conference (ACC)*. IEEE, 2021, pp. 178–185.

[24] A. Li, C. G. Cassandras, and W. Xiao, "Safe optimal interactions between automated and human-driven vehicles in mixed traffic with event-triggered control barrier functions," *arXiv preprint arXiv:2310.00534*, 2023.